sustainability

MDPI

Article

Distribution Pattern and Enrichment Mechanism of Selenium in Topsoil in Handan Se-Enriched Belt, North China

Huidi Hao [1], Minmin Zhang [1,2], Jinxi Wang [1,2,3,*], Shuting Jiang [1], Juanjuan Ma [1], Yafan Hu [1], Hongya Niu [1,2], Balaji Panchal [1,4] and Yuzhuang Sun [1,2]

[1] Key Laboratory of Resource Exploration Research of Hebei Province, Hebei University of Engineering, Handan 056038, China; 17853463993@163.com (H.H.); HUEZhangMM@126.com (M.Z.); j17395679923@163.com (S.J.); mj_pod@163.com (J.M.); hyf3052712573@163.com (Y.H.); niuhongya@hebeu.edu.cn (H.N.); panchalbalaji@yahoo.co.in (B.P.); syz@hebeu.edu.cn (Y.S.)
[2] College of Water Conservancy and Hydroelectric Power, Hebei University of Engineering, Handan 056038, China
[3] School of Resources and Geosciences, China University of Mining and Technology, Xuzhou 221116, China
[4] Nurture Earth R and D, Maharashtra Institute of Technology, Aurangabad 431010, India
* Correspondence: wangjinxi@hebeu.edu.cn

Abstract: Selenium (Se) is an essential trace element for human health with crucial biological functions. In this study, Se concentrations and physicochemical properties of soils in central and western Handan were determined to investigate their spatial distribution, enrichment degree, influencing factor, and geological source. The results show that: (1) Se concentrations vary from 0.00 to 1.95 μg/g, with an average of 0.45 μg/g, which exceed the mean of Se in soils in China (0.29 μg/g) and Hebei Plain (0.21 μg/g). (2) A continuous and irregular ring-like area showing significant enrichment of Se could be identified in Handan city, Yongnian District, Wu'an City, and Fengfeng Mining District. It can be defined as a positive abnormal Se zone, which is mainly located in the hilly area in the west of Handan City and east of Taihang Mountains, and the plains near Handan City. (3) Comprehensively, Se enrichment in the soil is principally affected by rock weathering, mining activities, and coal combustion. (4) As far as the single-factor pollution index (SFPI) is concerned, most of the study areas are in the safety domain and slightly polluted domain and are at low ecological risk. According to the Nemerow integrated pollution index (NIPI), the moderately and seriously polluted domain are distributed in Handan City, Fengfeng Mining District, and other central areas.

Keywords: geochemistry; selenium; spatial distribution; influencing factors; Handan; North China

Citation: Hao, H.; Zhang, M.; Wang, J.; Jiang, S.; Ma, J.; Hu, Y.; Niu, H.; Panchal, B.; Sun, Y. Distribution Pattern and Enrichment Mechanism of Selenium in Topsoil in Handan Se-Enriched Belt, North China. *Sustainability* **2022**, *14*, 3183. https://doi.org/10.3390/su14063183

Academic Editor: Franco Ajmone Marsan

Received: 14 January 2022
Accepted: 5 March 2022
Published: 8 March 2022

1. Introduction

Selenium is an essential micronutrient for organisms [1,2] and an integral component of the enzyme glutathione peroxidase (GSH-Px), which plays a pivotal role in energy metabolism and gene discovery [3]. It also possesses a wide spectrum of pleiotropic biological activities, including antioxidant, regulatory protein, and heavy metal antagonistic effects against mercury, lead, and cadmium [4]. The main manifestation is that heavy metals could limit the biological functions of antioxidant enzymes in the organism and destroy biofilms, while Se can slow down the toxic effects than heavy metals and improve the immunity system of the human body and resistance of the animals and plants [5]. Several reports showed that Se deficiency could induce Keshan disease and Kaschin–Beck disease [1,6], whereas excessive Se intake in the human body can result in selenosis, which symptoms include alopecia, nail removal, skin injury, and abnormal nervous system [1,7]. Therefore, appropriate daily intakes should be maintained for humans and animals. The Food and Agriculture Organization (FAO) and the World Health Organization (WHO) [8] recommend a limited threshold range of Se intake of 40 ug/d and 30 ug/d for men and women, respectively.

Selenium is widespread in a variety of environmental media (including rocks, soils, plants, and aquatic systems) through volcanic activity, rocks and soils weathering, fossil fuel burning, minerals precipitation, chemical or bacterial redox reactions, and animal metabolic absorption [9]. As a rare nonmetallic element, Se is distributed unevenly in the earth crust; the spatial distribution of Se in soils is also heterogeneous and variable. The mean of Se concentration in soils in the world ranges from 0.01 to 2.00 μg/g, with an average of 0.40 μg/g [1]. On the contrary, Se concentration in soils with a high geological background value of Se can reach 1200 μg/g [10]. Globally, the occupied area of soils with Se deficient is considerably more than that with high Se content. The background value of Se in soils in China is 0.29 μg/g, and 72% of the zones are classified as low and deficient levels. China was divided into six regions such as East China, Central-South China, North China, Northwest China, Northeast China, and Southwest China, with Central-South China having the highest average Se content in soils at 0.308 μg/g, and North China having the lowest at 0.180 μg/g [11].

The Se-deficiency belt is widely distributed in China, and the level of Se-deficient is high. Hebei Province is located in a Se-deficiency belt with a Se eco-geochemical reference value was 0.19 μg/g, especially an obvious Se-deficiency belt that appears in eastern Hebei Plain [12]. According to the result of a multi-objective regional geochemical investigation conducted by Hebei Province Geological Survey, Handan is generally in the Se-deficiency range, but several small regions exhibit Se-enrichment within soils, such as Cixian County, Yongnian District, Wu'an City [13]. It was found that the Se anomaly is liable to occur in specific ecological environment areas, mainly in coal-burning areas and mining areas.

Previous research revealed that anthropogenic pollution, notably atmospheric precipitation from local power plants and industry, was responsible for the positive anomaly of Se in central Hebei Province [14]. In addition, anomalies such as Hg, Pb, Zn, Cd, Ag, Sb, and TOC are associated with Se anomalies. Because of the weathering of high-Se layers, Se concentrations in the environment are strongly connected to those in exposed rock [15,16]. It is well established that elevated concentration of Se trended to occur in black rock series, such as Precambrian in Ziyang, Shaanxi Province [17], and Maokou Formation of Permian in Enshi, Hubei Province [18]. There are also coal-bearing dark classic rock series outcrops in the study area (Taiyuan Formation and Shanxi Formation), which are likely to provide Se sources for environmental media, including topsoil. Still, the source of Se has not been studied in more detail and depth. Therefore, it is necessary to supplement the basic data of Se in soils in Handan.

The objectives of the current study are to (1) determine the concentration and distribution patterns of Se in soils in Handan based on analyses for geochemical characteristics of collected 192 soil samples; (2) analyze the spatial distributions of Se on the basis of ecological landscape classification standard of Se in China [19] and considering the unique situation of the study area; (3) identify the physicochemical properties of soil and establishing a link between Se and other variables; (4) and analyze the enrichment factors of Se in soils of each county and finally identify the source of Se, to offer a solid basis for the rational development of Se-enriched soils and regional agricultural growth.

2. Geological Setting

The research study area is located in the south of Hebei Province, China (Figure 1A). The target area in this study focuses on the central and west of Handan (Figure 1B). Handan is situated at the eastern foot of the Taihang Mountains, with high terrain in the west and low in the east [20]. The landform types in this area are complex, which can be subdivided into western mountains, central hills, and eastern plains from west to east. During Yanshanian, the activities of the Pacific plate replaced those of the ancient Siberian plate and the ancient Yangtze plate, which brought about Chinese mainland to subduction relatively eastward, so that the eastern part of China was in a huge area with strong tensile stress; thus, a series of NNE (north–north-east)-trending continental rift belts and faulted basins were formed, such as Songliao, North China and Fenwei Rifts. The NNE-trending

faults in the study area occur in Yongnian–Cixian, Zi Shan–Yigushan, Kuangshan–Cixian, Longwu–Nancongjing, and Changting–Shexian [21].

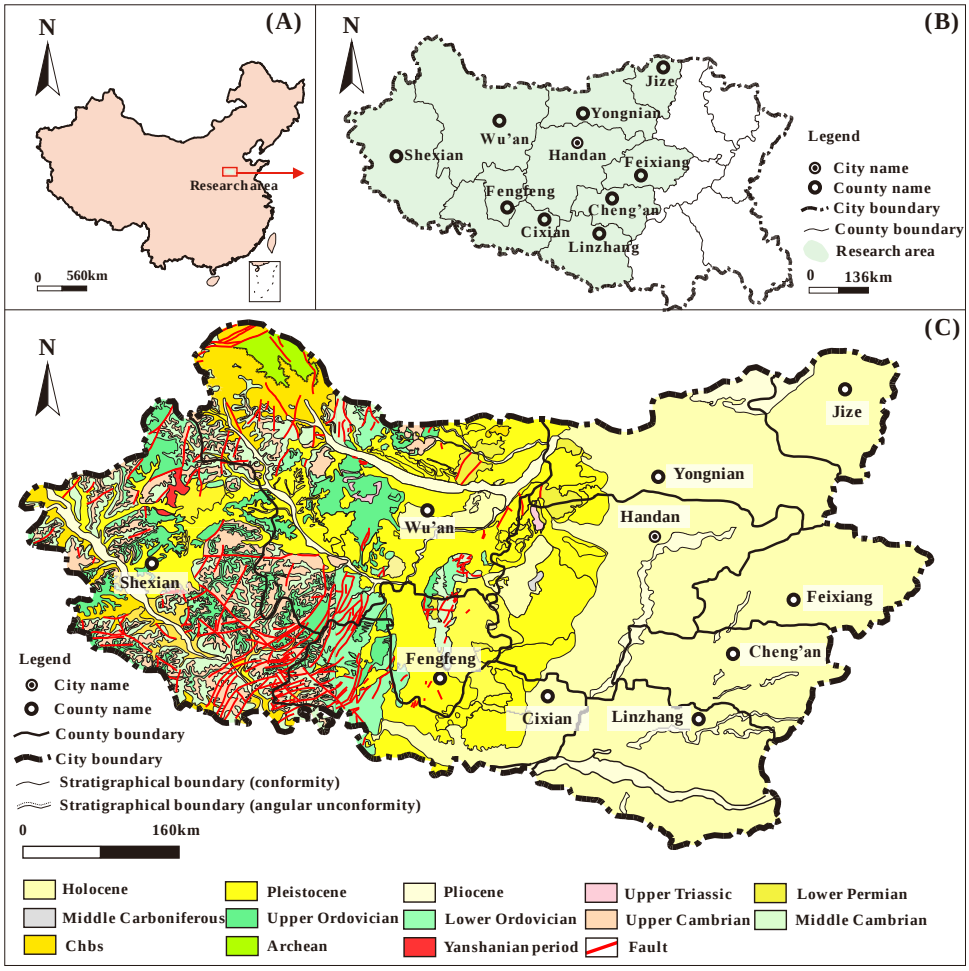

Figure 1. (**A**) Map of the research area in China; (**B**) Map of the research area in Handan area; (**C**) Research area geological map (modified after CGS, NGA).

The outcropped strata are mainly scattered on the mountainous and hilly areas in the west of Handan, Hebei Province [22]. The sequence of strata is from Archean to Quaternary. The terranes are mostly Paleozoic in age, with Cambrian, Ordovician, Carboniferous, and Permian strata (Figure 1C). The basement is Archean Zanhuang group gneiss, which is overlapped by the sedimentary cover of Cambrian–Ordovician marine carbonate rocks and Carboniferous–Permian coal-bearing clastic rocks [23]. The piedmont proluvial fan plain is dominated by diluvial or ice water accumulation, the upper part is loess loam, and the lower part is thick gravel, the central alluvial plain is an alternating alluvial and lacustrine deposit.

3. Materials and Methods

3.1. Sample Collection

The soil sample collection procedure adhered to Chinese national standard GB/T 36197-2018 (2018) and industry-standard DZ/T 0258-2014 (2014). To summarize, the grid sampling method was employed to collect topsoil samples, and the geographic coordinate information was recorded using a global positioning system (GPS). Five subsamples were taken (one from the center and four from the corners) within a 10 m × 10 m radius of each sampling site. Each topsoil sample was consisted of five subsamples, with a depth of 3–15 cm. A total of 192 samples were collected from September to November 2020. The

sampling sites were away from obvious point pollution areas and garbage dumps. In addition, weeds and fallen leaves on the surface layer were removed, and debris such as animal and plant residues and gravel were discarded. Subsequently, all samples were sealed in polyethylene bags with the right sample numbers and labels and then delivered to the laboratory for further investigation. The spatial distributions of sampling sites are shown in Figure 2A.

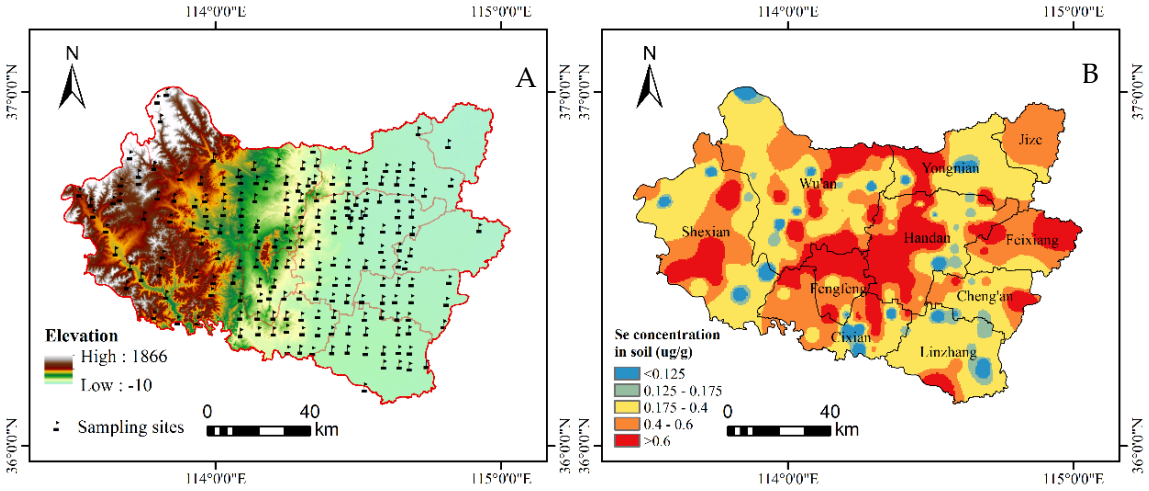

Figure 2. (**A**) Spatial distributions of sampling sites; (**B**) Spatial distribution of Se concentration in soils of research area.

3.2. Measurement Procedure

In the laboratory, soil samples were mixed uniformly after removing stones and other contaminants, then air-dried at room temperature (approximately 25 °C) before being sieved through 20-mesh (0.833 mm) (GB/T 6005-2008) and 200-mesh (0.074 mm) (GB/T 6005-2008) sieves. The flow chart containing the research contents and methods is shown in Figure 3.

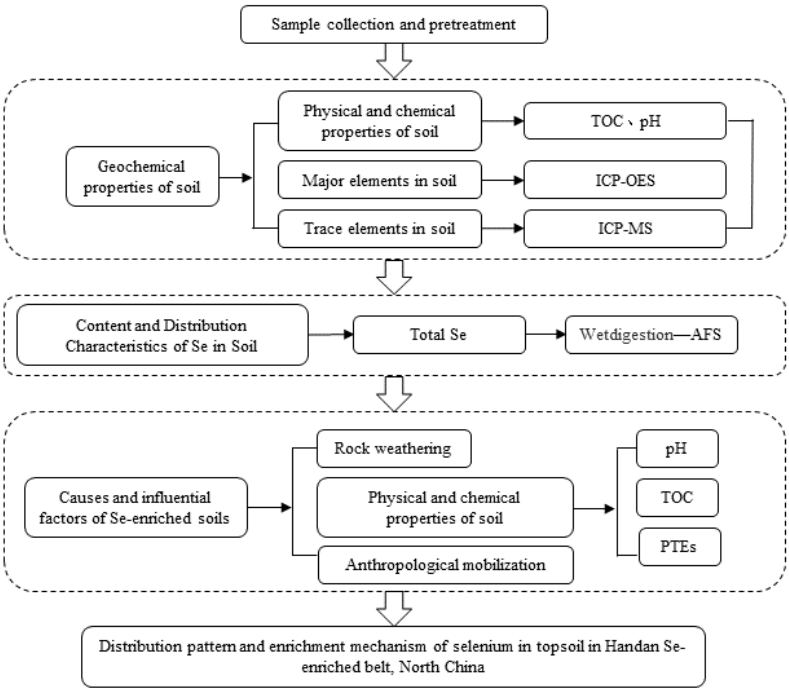

Figure 3. Flow chart of research contents and methods.

Before the analysis of the instrument, the soil samples should be digested. The dissolution mechanisms for major and trace elements analyses referred to Luo [24] and Tian et al. [25]. The schematic diagram of the experimental process of measuring major and trace elements is shown in Figure 4. The Se and arsenic (As) dissolution methods referred to Niu and Luo [26] and Ni et al. [16]. Unlike the measurement of major and trace elements, a 10 mL HNO_3-$HClO_4$ mixture (5:1 v/v) was pre-digested overnight in a 100 mL glass beaker. When $HClO_4$ vaporized, 3 mL HCl (6 mol/l) was added to the digested solution, and the glass beaker was reheated for 10 min. Ultimately, 1 mL HCl (12 mol/l) was added to the digested solution, and both were diluted with 25 mL ultra-pure water for Se and As concentration determination.

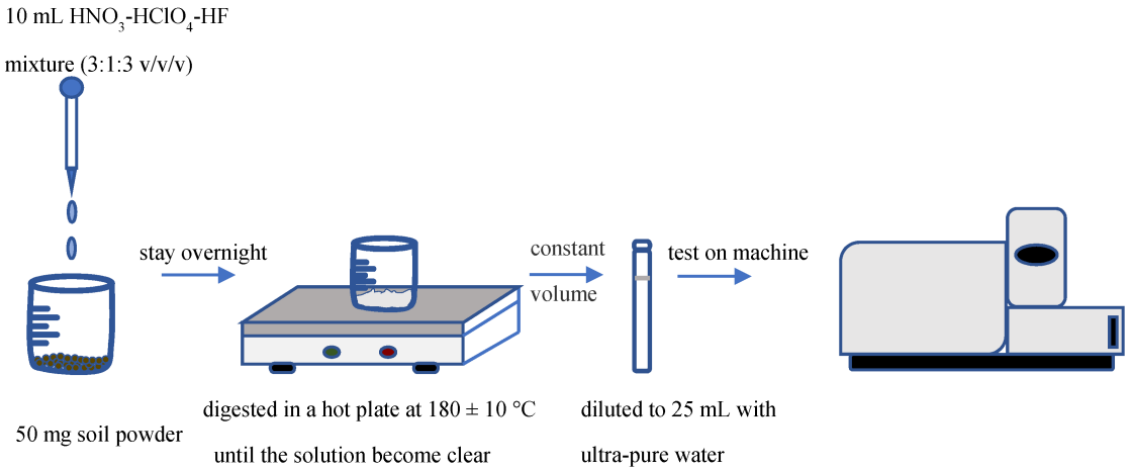

Figure 4. Schematic diagram of major and trace elements measurement process.

ICP-MS (detection limit is 0.001 g/L) and ICP-OES (detection limit is 0.001 mg/L) were used to determine the concentrations of trace and major elements, while As and Se were determined using a hydride generation atomic fluorescence spectrometer (HG-AFS 8220 Beijing Titan, the detection limit is 0.01 g/L). Blank experiments, duplicate samples, and national standard reference materials (GBW07110 and GBW07403) were used to test the accuracy and precision of the dissolution and subsequent measurement. The recoveries of standard materials were controlled within 90–105%, and the relative standard deviation (RSD) of duplicated samples was less than 10%.

The measurement for TOC is as follows: firstly, cleaned-up porcelain crucibles were burned at 350–380 °C for 1 h using a muffle furnace, then taken out and placed in a desiccator for cooling at room temperature, and the porcelain crucible (m_0) was weighted after it was constant in weight. Secondly, the soil samples with the volume of about half of the crucible were loaded, weighed again (m_1), and dried in an oven (105 °C, 8 h). The sample crucibles were removed into a desiccator rapidly after drying. Then the porcelain crucibles were weighed (m_2) until dropping to room temperature, and the water content was calculated. Thirdly, the dried samples with the porcelain crucibles were put into a muffle furnace together and burned at 380 °C for 1 h, and then crucibles were removed into a desiccator rapidly when the furnace fell to 100–150 °C. Then the porcelain crucibles were weighed (m_3) until dropping to room temperature and calculated the organic matter content. The value of TOC was calculated by the formulas:

$$\text{The water content}(\%) = \left(\frac{m_1 - m_2}{m_2 - m_0}\right) * 100 \quad (1)$$

$$\text{SOM}(\%) = \left(\frac{m_2 - m_3}{m_3 - m_0}\right) * 100 \quad (2)$$

$$\text{TOC}(\%) = \text{SOM}/1.724 \quad (3)$$

The coefficient of weathering and eluviation (BA) [27] is introduced as an equation to represent the leaching degree of soil base ions:

$$BA = (CaO + MgO + Na_2O + K2O)/Al_2O_3 \quad (4)$$

3.3. Calculation of Pollution Indices

The potentially toxic in the soil was assessed using the single-factor pollution index (SFPI) and the Nemerow integrated pollution index (NIPI).

$$P_i = C_i/S_i \quad (5)$$

where P_i is the SFPI of heavy metal element i, and C_i and S_i represent the measured and the background concentration of heavy metal i, respectively. Trace elements concentration in Eastern China plain (ECP) [28] was selected as the background concentration.

A comprehensive evaluation of soil environmental quality adopted a single integrated pollution index [29] to work out the comprehensive pollution index, whose results not only considered the average level of pollution of different pollutants but also reflected environmental damage caused by the most polluting pollutant. Its equation is as follows:

$$P_n = \sqrt{\frac{\left(\overline{P_i}\right)^2 + \left(P_{imax}\right)^2}{2}} \quad (6)$$

P_n is the NIPI, and $\overline{P_i}$ and P_{imax} are the mean and maximum of all PTEs pollution indices, respectively. P_n was calculated for all soil sampling points to show the relative extent of soil contamination. P_n with a higher value implies more hazardous pollution. Chen [30] proposed the SFPI and NIPI categorization criteria in Table 1.

Table 1. Criteria for classifying contamination indexes of soil environmental quality.

Degree	SFPI		NIPI	
	P_i	Pollution Level		Pollution Level
I	$P_i \leq 1$	Safety domain	$P_n \leq 0.7$	Safety domain
II	$1 < P_i \leq 2$	Slightly polluted domain	$0.7 < P_n \leq 1$	Precaution domain
III	$2 < P_i \leq 3$	Moderately polluted domain	$1 < P_n \leq 2$	Slightly polluted domain
IV	$3 < P_i$	Seriously polluted domain	$2 < P_n \leq 3$	Moderately polluted domain
V	-	-	$3 < P_n$	Seriously polluted domain

3.4. Statistical and Analytical Analysis

Pearson's correlation analysis and principal component analysis (PCA) were performed using IBM® SPSS® Statistics software version 22.0. Through Pearson's correlation, the relationship between two variables (elements) was determined because this relationship often shows the information of material sources. Origin (version 2018C) was employed to make a point-fold line chart. ArcGIS (version 10.2) was employed to input GPS coordinate of sampling sites and create a special gradient of trace elements concentration and other parameters. Acquisition of 30 m resolution Digital Elevation Model (DEM) data from the China Geospatial Data Cloud. DEM was inserted into the distribution map of sampling points to objectively and clearly show the change in topography in the study area. The spatial distribution of Se content and the contamination distribution of PTEs in the study area were explored using inverse distance weight interpolation. The closer the discrete point is to the interpolation point, the greater the weight given to the discrete point [31].

4. Results and Discussions

4.1. Geochemical Characteristics of Soil Samples

4.1.1. Major and Trace Elements Concentrations

Tables S1 and S2 in the Supplementary Materials list the concentrations of major and trace elements in soil samples, respectively. Statistics of soil geochemical parameters in the study area are listed in Table 2. Compared with the China soil abundance [32], the elements with higher soil background values in the study area: major elements are SiO_2, CaO, Fe_2O_3, MgO, and P_2O_5; potentially toxic trace elements Cu, Pb, and Zn; and rare earth elements are La, Ce, Nd, Sm, Eu, Gd, and other elements. By comparing the background value of soil elements with the reference value of the plain of Eastern China (ECP) [28], we can conclude that oxide CaO, Fe_2O_3, MgO, and P_2O_5 are higher than the reference value of ECP, and CaO is 1.4 times higher than that of ECP values. Elements with low background values in soils include alkaline earth metals Sr and Ba and alkali metals Li, Na, K, and Cs. It is speculated that the strong leaching of acid soil factors in the loss of alkali metal and alkaline earth metal elements. In particular, elements with abnormally high background values in soils are S (6.1 times higher than that of Chinese soils, 5.8 times higher than that of ECP), Se (2.25, 4.5), and Ge (3.6, 3.3), while elements that are significantly lower than the reference value are As (0.39, 0.39), Nb (0.12, 0.13), Sn (0.33, 0.26), and Hf (0.05, 0.04).

Table 2. Statistics of geochemical parameters in soil.

	Avg	Range	China [32]	ECP [28]		Avg	Range	China [32]	ECP [28]
Li	33.19	8.10–201.57	30	36	Mo	1.30	0.06–3.63	0.80	0.57
Be	2.74	1.18–6.69	1.80	2.30	Cd	0.27	0.08–1.29	0.09	0.12
Na_2O	1.52	0.81–2.12	1.60	1.63	In	0.07	0.02–0.22	0.06	0.05
MgO	1.91	0.82–11.27	1.80	1.57	Sn	0.82	0.02–11.08	2.50	3.10
Al_2O_3	10.85	4.55–18.94	12.60	13.51	Sb	0.71	0.07–2.10	0.80	0.79
SiO_2	65.16	41.50–80.98	65	66	Cs	6.66	1.50–10.78	7	7.50
P_2O_5	0.18	0.01–0.53	0.12	0.10	Ba	417.16	193.05–814.93	500	565
S	921.82	129.86–6205.69	150	159	La	40.79	11.97–97.31	38	37
K_2O	2.32	0.90–3.24	2.50	2.47	Ce	80.67	25.09–200.60	72	58
CaO	4.09	0.84–16.87	3.20	2.91	Pr	9.24	2.66–22.49	8.20	7
Sc	11.21	3.32–16.23	11	11	Nd	33.66	9.86–80.37	32	27
TiO_2	0.58	0.04–1.00	0.72	0.72	Sm	6.10	1.92–13.54	5.80	5.20
V	78.04	8.46–165.26	82	87	Eu	1.31	0.41–1.96	1.20	1.12
Cr	60.63	25.32–129.57	65	65	Gd	5.60	1.79–11.90	5.10	4.50
MnO	0.07	0.03–0.26	0.08	0.09	Tb	0.77	0.25–1.46	0.80	0.73
Fe_2O_3	4.20	1.58–11.31	3.40	3.89	Dy	3.90	1.27–6.55	4.70	3.90
Co	16.08	5.60–105.11	13	13	Ho	0.75	0.25–1.20	1	0.92
Ni	34.86	13.23–278.15	26	30	Er	2.24	0.74–3.56	2.80	2.40
Cu	29.40	7.36–360.96	24	23	Tm	0.31	0.10–0.49	0.42	0.42
Zn	85.42	23.30–253.72	68	64	Lu	0.31	0.10–0.48	0.40	0.39
Ga	18.40	6.64–38.73	17	15.70	Hf	0.36	0.01–2.34	7.40	8.50
Ge	4.72	1.78–8.21	1.30	1.42	Ta	0.11	0.00–0.78	1.10	1.17
As	3.89	0.95–8.49	10	10	W	0.65	0.02–3.78	1.80	1.70
Se	0.45	0.00–1.95	0.20	0.10	Tl	0.55	0.18–0.78	0.60	0.66
Rb	113.89	54.06–154.77	100	107	Pb	29.03	11.01–99.83	23	23
Sr	170.47	89.63–433.65	170	173	Bi	0.20	0.00–1.23	0.30	0.31
Y	22.02	6.70–35.91	23	26	Th	10.38	0.97–30.74	12.50	12
Zr	19.27	0.07–121.62	250	251	U	2.32	0.79–6.11	2.60	2.30
Nb	1.94	0.02–12.85	16	15.50					

The unit of oxide content is %, the unit of rest elements is μg/g; Avg = Average.

4.1.2. Total Se Concentrations

The properties of the soil samples and concentrations of total Se are presented in Table 3. Total Se concentrations in Handan area soils range from 0.00 to 1.95 μg/g. The mean is 0.45 μg/g, which exceeds the threshold of Se-enrichment (0.40 μg/g) proposed

by Tan [19] in 1989 and is significantly higher than the average value of soil Se in China (0.29 μg/g) [33] and Hebei plain (0.21 μg/g) [12]. The standard deviation of total Se in the research area is 0.36, and the coefficient of variation is 0.80, which is 3.08 times China's standard deviation (0.26) [34] and 0.89 times China's coefficient of variation (0.90) [34].

Table 3. Soil properties and concentrations of total Se and As.

	Total Se (μg/g)	pH	TOC
Mean	0.45	7.10	1.44
Median	0.33	7.13	1.37
Range	0.00–1.95	6.28–7.67	0.30–3.10
Standard deviation	0.36	0.25	0.50
Coefficient of variation	0.80	0.04	0.35

Tan [19] proposed, based on the ecological landscape classification standard of Se in China, the interval of 0.4–0.6 μg/g was added to the original standard according to the fact of the study area in order to divide the level of high Se concentration further [35] (Table 4). In the study area, Se-enrichment and Se-moderate categories are depicted as the dominant ones in about 48.4% and 39.7% of the total soil area, respectively, followed by Se-deficient (6.1%) and Se-marginal (2.96%). However, there is no Se-excessive in this research, indicating that there are a few potential risks of selenosis in the soils.

Table 4. Threshold between abundance and deficiency of soil Se.

Category	Se Concentration (μg/g)	Area (km^2)	Proportion (%)
Se-deficiency	<0.125	776.6	6.1
Se-marginal	0.125–0.175	741.2	5.8
Se-moderate	0.175–0.4	5064.3	39.7
Light Se-enrichment	0.4–0.6	3307.5	25.9
High Se-enrichment	0.6–3	2861.1	22.5
Se-excessive	>3	0	0

4.1.3. Distribution Pattern of Se in Soils

The distribution of Se enrichment in soil shows an obvious aggregation, as shown in Figure 2B. The concentration of Se in the central region of the target area is obviously higher than the surrounding region, especially in the middle and west of Handan City and in the northern part of Fengfeng Mining District. A continuous and irregular ring-like area is formed in Handan City, Yongnian District, Wu'an City, and Fengfeng Mining District. We defined this high Se-enrichment area as the positive abnormal Se zone, which is mainly located in the hilly area in the west of Handan City, the east of Taihang Mountains, and the plains near Handan city. In addition, minor areas with high Se-enrichment concentration are scattered in Feixiang County, Cheng'an County, Linzhang County, and Shexian County. The light Se-enriched area is mostly clustered around the high Se-enrichment area. Soil with Se-moderate concentration occupies the largest area in the map, which usually acts as a buffer zone between Se-enrichment and Se-deficient area. Se-deficiency areas are scattered in the study area and have not yet reached a certain scale.

Combining geological map with a spatial distribution map of Se concentration, the high Se-enrichment area has the highest coincidence degree with Carboniferous–Permian period, while the Se-deficiency area has no obvious preference in geological distribution. In addition, the distribution of Se in soils could be indirectly affected by topography through the redistribution of minerals, water, and energy in soils [36]. Normally, the Se concentration in the soil of flat terrain has relatively enrichment [37]. Similarly, a large area of Se enrichment in this study is located in plain and low hilly areas. However, in the western mountainous areas with higher altitudes, there is also a small area of Se enrichment, which is supposed to be caused by weathering and erosion of exposed strata.

4.2. Enrichment Factors of Se in Soils

Enrichment factor (EF), the ratio of elemental concentration in soils to the average arithmetic value of corresponding element concentrations in the Upper Continental Crust (UCC) [38], was used as an index reflecting the enrichment level. The values of EF are divided into five classes to portray the degree of enrichment of elements in this study: depleted (EF < 0.5), normal (2 > EF > 0.5), slight enrichment (10 > EF > 2), strong enrichment (100 > EF > 10), anomalous enrichment (EF > 100). EF values of Se vary greatly from 0.01 to 21.66, with an average of 5.06. Due to the multitudinous data, the enrichment degree of trace elements in soil samples is presented according to each county. The degree of Se enrichment in each county is slight enrichment; the maximum EF of Se is in Handan, Shexian, and Fengfeng, while the minimum value is in Wu'an, Shexian, and Cixian (Table 5). The mean and maximum values of Se EF in Handan and Fengfeng are ranked at the forefront among all the counties.

Table 5. Se and EF values in soils samples in different countries.

	YN (n = 18)		WA (n = 42)		SX (n = 25)		LZ (n = 15)		FF (n = 11)		FX (n = 5)		CX (n = 22)		CA (n = 13)		JZ (n = 1)		HD (n = 41)	
	Se	**Se_{EF}**	**Se**	**Se_{EF}**	**Se**	**Se_{EF}**	**Se**	**Se_{EF}**	**Se**	**Se_{EF}**	**Se**	**Se_{EF}**	**Se**	**Se_{EF}**	**Se**	**Se_{EF}**	**Se**	**Se_{EF}**	**Se**	**Se_{EF}**
Avg.	0.36	3.98	0.41	4.60	0.41	4.60	0.21	2.28	0.75	8.37	0.46	5.13	0.45	5.03	0.35	3.93	0.57	6.33	0.57	6.35
Max.	1.07	11.90	1.25	13.84	1.77	19.64	0.47	5.22	1.80	19.98	0.69	7.71	1.21	13.43	0.85	9.40	0.57	6.33	1.95	21.66
Min.	0.08	0.89	0.00	0.01	0.00	0.01	0.02	0.26	0.12	1.33	0.26	2.84	0.00	0.01	0.12	1.34	0.57	6.33	0.05	0.53

Avg. = Average, Max. = Maximum, Min. = Minimum, YN = Yongnian, WA = Wu'an, SX = Shexian, LZ = Linzhang, FF = Fengfeng, FX = Feixiang, CX = Cixian, CA = Cheng'an, JZ = Jize, HD = Handan.

The top nine EF mean values of trace elements are: S (14.87) > Se (4.97) > Ge (3.37) > Cd (2.99) > Sb (1.77) > Pb (1.71) > Li (1.38) > Cs (1.36) > Rb (1.36). Sulfur is strong enrichment, Se, Ge, and Cd manifest slight enrichment, and the rest four are normal. EF values of Ge, Rb, Cs, and Sb exhibit a great variation in different counties, while EF values of Li, S, Cd, and Pb are relatively stable (Figure 5). The enrichment level of S in the study area is the highest. Except for Linzhang and Cixian, the enrichment level of S in other counties is strong enrichment, and Wu'an even reaches anomalous enrichment. Selenium is a sulphophil, and the enrichment of S affects the enrichment of Se to some extent.

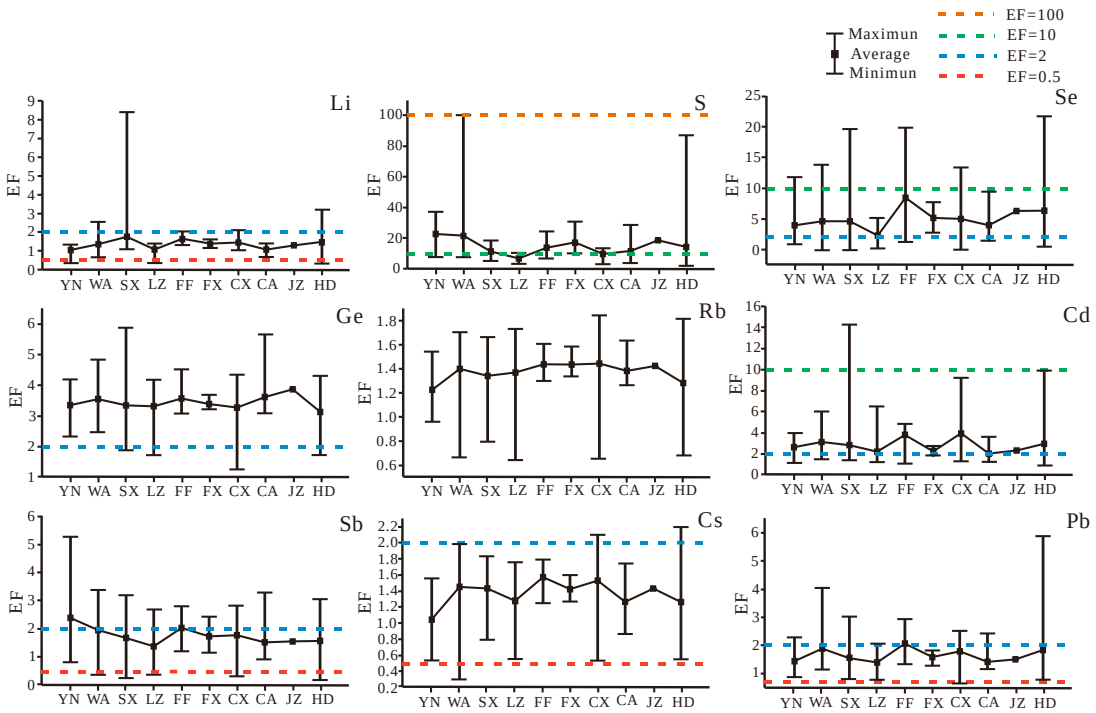

Figure 5. Variation in EF values of trace elements.

4.3. Physicochemical Properties of Soils

4.3.1. pH, TOC, and BA

The study results found that the migration and dissolution of Se largely depend on the adsorption/desorption reaction, pH, organic–inorganic complexion, and the dissolution process in soils and sediments [39–42]. Typically, excessive Se areas (Se $\geq$ 3.0 μg/g) are dominated by black shales, such as Enshi, Hubei Province [37] and Taoyuan, Hunan Province [16]. However, the influence of soil physicochemical properties on Se concentration appears to increase as soils are formed [43]. While parent materials play an important role in excessive Se in soil, soil physicochemical properties also play a role in Se-enriched soil. The pH and TOC values in soil samples are listed in Table S3 (Supplementary Material). On chosen major and trace components in soil samples, Pearson's correlation matrix analysis was performed (Table 6).

Se main forms are present in soils such as selenide, organic selenide, selenite, selenate, etc. Soil pH is one of the significant factors controlling the transformation between selenite and selenate. Generally, Se principally exists as selenite (SeO_3^{2-}) under acidic and neutral conditions, which is easily adsorbed and fixed on the hydroxide of aluminum, iron, or manganese in the soil, with weak migration and leaching action [44]. However, in well-ventilated alkaline soils, selenate (SeO_4^{2-}) is the most common form of Se, which is not easily fixed by metal oxides and has strong mobility and solubility. Although the higher the soil pH, the easier the leaching loss of Se and the lower the Se concentration. Previous investigations in China have shown that pH negatively affects Se sorption in soils; Se sorption diminishes with expanding pH [45–47]. The correlation coefficient between Se concentration and pH value is 0.001 ($p > 0.05$) in our analysis, demonstrating that pH is not the key factor affecting Se concentration distribution. Previous reports suggested no significant correlation between pH and Se concentration [48–50]. The results suggest that the effect of pH on soil Se concentration could not be generalized, and further research on pH is necessary.

Many studies found that TOC and Se concentrations are closely related in soil; Se concentrations are generally high in organic-rich soil, e.g., dark brown loam and black soil in northeast China [51], which is in accordance with the result of this study. The correlation coefficient between Se concentrations in soils and TOC value is 0.228 ($p < 0.01$), indicating a significant positive correlation between them. Soil organic compounds play a key role in regulating the biological effectiveness of Se. In organic-rich soils, Se can preferentially enter the low-molecular-weight humus components, present an inorganic composite state compounded with metal humus, and be fixed in the soil. To a certain extent, TOC has a huge explicit surface region and a solid chelating capacity [52]. With the increase in total organic carbon, the adsorption and fixation of Se in soil are strengthened so that Se is rapidly fixed and accumulated in topsoil [53].

Chen et al. [54] investigated stronger degrees of leaching are linked to smaller values of BA, as Al_2O_3 is more stable than alkali ions. Despite the fact that there is no significant correlation between Se and BA, Se in soils exhibits significantly positive correlation with Al_2O_3 (r = 0.230, $p < 0.01$), and negative correlation with MgO (r = −0.184, $p < 0.05$), Na_2O (r = −0.168, $p < 0.05$), whereas show no significant correlation with CaO, K_2O. However, BA has a significantly negative correlation with TOC (r = −0.245, $p < 0.01$). These results indicate that bastions (CaO, MgO, Na_2O, K_2O) affected soil Se concentration by influencing the soil TOC. In addition, BA has a significantly negative correlation with Al_2O_3 (r = −0.523, $p < 0.01$), while Se and Al_2O_3 have a significantly positive correlation, indicating that BA indirectly affects Se by affecting Al. Moreover, no significant relationship exists between Se and P. Generally, the application of P fertilizer in agricultural activities can bring about an increase in Se concentration in soils [55]. Our study results imply that the Se concentrations in soils o are less affected by the application of phosphate fertilizer.

Table 6. Correlation between soil Se concentration with other properties.

	Se	pH	TOC	As	Cd	Pb	Cr	Ni	Cu	Zn	SiO_2	Al_2O_3	CaO	Fe_2O_3	K_2O	MgO	MnO	Na_2O	P_2O_5	L	BA
Se	1																				
pH	0.001	1																			
TOC	0.228 **	−0.148 *	1																		
As	0.036	−0.004	−0.031	1																	
Cd	0.282 **	−0.124	0.162 *	0.033	1																
Pb	0.454 **	−0.135	0.196 **	0.067	0.656 **	1															
Cr	0.144 *	0.048	0.157 *	0.055	0.101	0.385 **	1														
Ni	0.150 *	0.027	0.221 **	0.016	0.113	0.207 **	0.222 **	1													
Cu	−0.031	−0.145 *	−0.018	0.018	0.058	0.080	0.168 *	0.186 **	1												
Zn	0.270 **	−0.239 **	0.213 **	0.039	0.351 **	0.438 **	0.307 **	0.217 **	0.383 **	1											
SiO_2	−0.055	0.062	−0.154 *	0.015	−0.100	−0.190 **	−0.347 **	−0.295 **	−0.550 **	−0.334 **	1										
Al_2O_3	0.230 **	0.065	0.300 **	0.007	0.082	0.295 **	0.286 **	0.136	−0.277 **	0.026	−0.261 **	1									
CaO	0.028	−0.116	−0.200 **	−0.029	0.147 *	0.189 **	0.120	0.139	0.636 **	0.347 **	−0.730 **	−0.175 *	1								
Fe_2O_3	0.128	0.052	−0.023	0.042	0.166 *	0.441 **	0.544 **	0.213 **	0.591 **	0.488 **	−0.601 **	0.097	0.566 **	1							
K_2O	−0.018	0.081	0.235 **	0.057	0.083	0.071	0.090	−0.012	−0.387 **	0.061	0.067	0.448 **	−0.240 **	−0.079	1						
MgO	−0.184 *	−0.079	−0.178 *	0.024	−0.026	−0.060	0.114	0.130	0.878 **	0.243 **	−0.618 **	−0.318 **	0.728 **	0.610 **	−0.298 **	1					
MnO	−0.098	0.019	−0.021	0.060	0.065	0.125	0.541 **	0.198 **	0.527 **	0.368 **	−0.596 **	−0.024	0.530 **	0.665 **	−0.110	0.628 **	1				
Na_2O	−0.168 *	0.049	−0.232 **	0.048	−0.092	−0.201 **	0.045	−0.090	−0.291 **	−0.117	0.291 **	0.040	−0.327 **	−0.159 *	0.343 **	−0.177 *	−0.111	1			
P_2O_5	0.030	−0.254 **	0.329 **	0.102	0.011	0.116	0.284 **	−0.061	0.181 *	0.341 **	−0.222 **	−0.021	0.071	0.248 **	0.062	0.109	0.156 *	0.109	1		
L	−0.018	0.180 *	0.357 **	0.106	−0.010	0.003	0.138	0.123	0.044	0.118	−0.247 **	0.326 **	−0.084	0.116	0.292 **	0.008	0.110	−0.118	0.071	1	
BA	−0.126	−0.110	−0.245 **	−0.013	0.006	−0.054	−0.014	0.087	0.878 **	0.236 **	−0.500 **	−0.523 **	0.788 **	0.486 **	−0.400 **	0.916 **	0.471 **	−0.233 **	0.071	−0.109	1

Note: * Correlation is significant at the 0.05 level (2-tailed); ** Correlation is significant at the 0.01 level (2-tailed); L = elevation.

4.3.2. Potentially Toxic Trace Elements

This study analyzed the correlation between potentially toxic trace elements (PTEs) of cadmium (Cd), lead (Pb), zinc (Zn), nickel (Ni), and chromium (Cr) in soils and Se concentrations in soils. As shown in Table 6, all PTEs except Cu are positively correlated with Se. The correlation between Cr and Ni with Se is significant, while the correlation between Cd, Pb, and Zn with Se is extremely significant. Selenium has the most obvious positive correlation with both Pb and Cd, with correlation coefficients of 0.454 and 0.282, respectively. The reason for the good correlation with PTEs and Se is that Pb, Cd, Cr, Zn, and other elements mostly exist in the form of sulfide, while the geochemical properties of Se are similar to those of S. Selenium and S are prone to isomorphism, while Pb, Zn, Fe, and Cu are similar in geochemical behaviors, such as galena, sphalerite, pyrite, and chalcopyrite.

Therefore, Se is easy to combine with the above metal elements in primary minerals to form compounds [56]. Later, in the process of rock weathering forming soils, the soil inherited the associated relationship of elements in primary minerals.

4.3.3. Driving Factors of Se Concentration

The driving factors for the spatial distribution of soil Se concentration in Handan are revealed and explained using principal component analysis (PCA). PCA is the multivariate analysis method that could be extensively applied to dimensionality decompositions and transform a high-dimensional set of connected variables into a low-dimensional set of unrelated variables [57,58]. Kaiser–Meyer–Olkin test (KMO > 0.6) and Bartlett's test of sphericity (Bartlett's test $p < 0.001$) were conducted in this study to ensure that PCA is applicable to analyze the data set of all the soil samples ($n = 192$). The first six-component eigenvectors can explain 69.679 percent of the entire variance, as shown in Table 7. Figure 6 shows a 3D loading plot of the first three principal components (PC1 vs. PC2 vs. PC3) to visualize the relationship with the elements being examined. PC1 shows strong positive loadings for Cu (0.857), MgO (0.918), CaO (0.829), BA (0.857) Fe_2O_3 (0.774), and MnO (0.778) and negative loadings for SiO_2 (−0.758). MgO, CaO, Al_2O_3, and BA are all tightly linked to pedogenic processes, indicating that the leaching of base ions is extremely [36]. It shows that the geochemical characteristics of soil in the Handan area are most affected by the following minerals: iron–manganese oxide minerals, metal minerals, and carbonate minerals. SiO_2 is considered to be an indicator of terrestrial aluminosilicate, a product of weathering processes [59]. PC2 shows strong positive loadings for Se (0.688), Cd (0.755), and Pb (0.881). Selenium-enriched soil is often associated with PTEs; a small amount of Se can exist in the form of selenides with Ag, Cu, Pb, Ni, and other metals. Selenium, Cr, and Pb are in the same group, and they are common sources of soil chemicals. The concentration of Cr in the soil in the study area is not enriched, and its average value is lower than the ECP background value. The content of Cr is probably due to the natural weathering and erosion of sedimentary rocks during the formation of the soil. Therefore, it can be inferred that Se in soil originates from weathering and deposition of exposed rocks to some extent. Additionally, PC2 shows positive loadings for Fe_2O_3 (0.298) and As (0.082), along with Se, Cd, and Pb, which are classified as siderophile and chalcophile that are abundant in mantle-derived magma [60]. PC3 is composed of TOC (0.718) and L (0.770), where L indicates the elevation. PC4 is formed of Cr (0.647) and Na_2O (0.618). PC5 is composed of pH (−0.719) and P_2O_5 (0.763). The aforementioned indicate that accumulation of biomass, acid, and alkaline features in soils impacted the soil Se concentration. PC6 shows strong positive loadings for As (0.928). The result of PCA shows that the spatial distribution of Se concentration in the topsoil of Handan is affected synthetically by siderophile and chalcophile Cd, Pb, Fe_2O_3, and As.

Table 7. Rotated component matrix for the examined elements in soil samples.

Elements	PC1	PC2	PC3	PC4	PC5	PC6
Se	−0.095	**0.688**	0.141	−0.078	−0.019	−0.024
pH	−0.012	−0.123	0.119	0.182	**−0.719**	0.112
TOC	−0.155	0.177	**0.718**	−0.029	0.439	−0.083
As	0.006	0.082	0.044	0.035	−0.007	**0.928**
Cd	0.029	**0.755**	−0.057	−0.006	0.091	0.080
Pb	0.111	**0.881**	0.053	0.170	0.074	0.004
Cr	0.354	0.268	0.149	**0.647**	0.050	−0.055
Ni	0.239	0.256	0.345	0.020	−0.146	−0.088
Cu	**0.857**	0.003	0.012	−0.247	0.178	0.063
Zn	0.391	0.472	0.102	0.148	0.426	0.070
SiO_2	**−0.758**	−0.097	−0.392	−0.096	−0.039	0.135
Al_2O_3	−0.199	0.247	0.543	0.479	−0.161	−0.169
CaO	**0.829**	0.150	−0.080	−0.165	−0.001	−0.077
Fe_2O_3	**0.774**	0.298	0.065	0.322	0.003	0.021
K_2O	−0.311	−0.015	0.294	0.564	0.041	0.094
MgO	**0.918**	−0.165	−0.079	−0.146	0.055	0.066
MnO	**0.778**	0.021	0.065	0.322	−0.005	0.018
Na_2O	−0.258	−0.260	−0.394	**0.618**	0.076	0.120
P_2O_5	0.156	−0.031	0.103	0.276	**0.763**	0.123
L	0.057	−0.125	**0.770**	0.123	−0.065	0.241
BA	**0.857**	−0.110	−0.218	−0.344	0.081	0.060
Eigenvalues	5.610	3.297	1.840	1.471	1.387	1.027
Explained variance (%)	26.716	15.699	8.763	7.006	6.606	4.889
Cumulative (%)	26.716	42.414	51.177	58.184	64.790	69.679

Bold: principal component analysis.

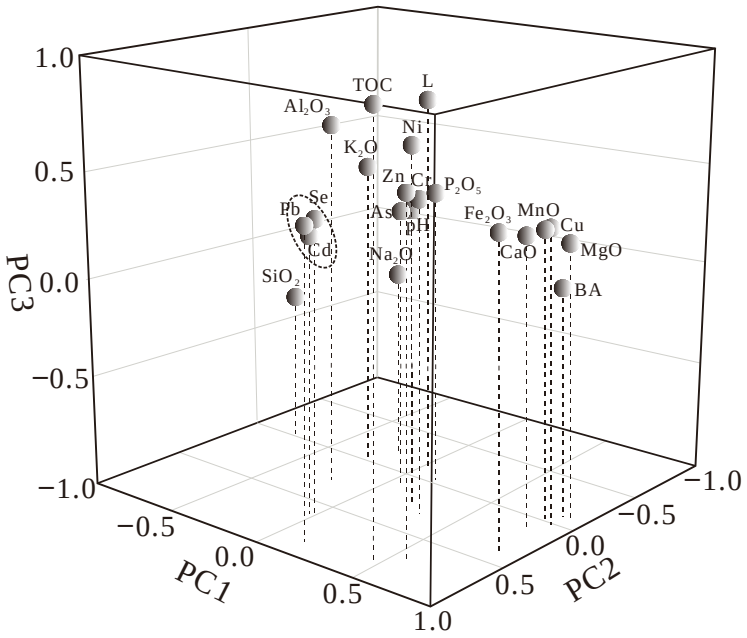

Figure 6. 3D-PCA loadings plot for first three rotated components for examined elements.

4.4. Source Apportionment for Se in Soils

The enrichment of Se in the soil is usually due to high geological background, secondary enrichment, anthropogenic input, and superposition of multiple effects. The influences from both anthropogenic factors (coal mining and coal combustion) and natural factors (weathering and leaching of rock) are considered in this study. Figure 7 illustrates the theoretical cycle of Se in soil, in which both natural and anthropological mobilization of Se sources are taken into account.

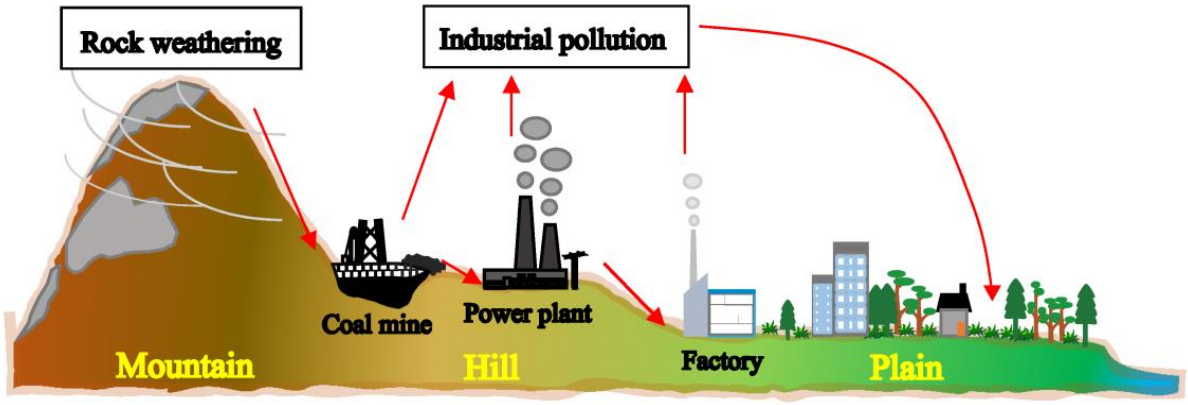

Figure 7. Source of Se in topsoil in Handan.

Outcropped rock erosion is recognized as a major source of Se in the soil, accounting for roughly 40% of the natural Se in the Earth's crust [61]. In the original geological environment, Se is mostly obtained from Se-enriched sedimentary rocks, such as black shale and coal measures layers [62]. Zhang et al. [63] proposed Se enrichment in the Mountain soil. In western Handan, the Zishan area is mostly influenced by rock weathering. Selenium enrichment belt in the study area is mainly located in the hilly area where strata of Carboniferous to Permian outcrop. In addition, a large area of dark rock series with a coal-bearing stratum of dark mudstone of Upper Carboniferous to Permian is outcropped in the Se anomaly zone. The Carboniferous to Permian is one of the most important periods of Se accumulation in sediments. For instance, Se concentrations in coal gangue from the Shanxi Formation of the Permian were found to range from 1.88 to 13.50 μg/g, with an average of 6.79 μg/g, in the Xishan Coalfield, Shanxi Province, China [64]. In Northumberland, Northeast England, carboniferous coal with a maximum Se content of 61.9 μg/g was observed. The highest Se concentration in Carboniferous coal in Northumberland of Northeast England was measured at 61.9 ug/g [65]. Sedimentary rocks and metamorphic rocks are the main rock types in Hebei Province. Generally, Se concentrations in sedimentary rocks are higher than in metamorphic rocks [66]. The soil in the mountain supergene zone is mostly formed by weathering of bedrock nearby, so the elemental characteristics of supergene soil are mainly determined by geological formation characteristics. As the concentration of Se in the rocks varies, so does the concentration of Se in the soil after weathering, transport, and soil formation.

Evidence shows that Se enrichment in soils has been linked to weathering and leaching of coal and gangue dump [67,68] or emission of coal combustion [69]. The abnormal Se zone in the research area coincides with the location of intensive coal mines and steel plants. It can be speculated that the main anthropogenic activities resulting in high Se concentration in Handan and Fengfeng are coal mining and combustion, which can result in the release of Se into the atmosphere and eventual deposition into the environment. Burning fossil fuels (e.g., coal) release significant amounts of Se in ashes, volatile compounds, and liquid effluents [70]. Selenium would be released by mining activities when mined rock and coal are exposed to snow, rain, and temperature variation [71]. Coal gangue is discharged in the process of coal mining, and coal washing also releases Se by leaching. The chemical composition of coal gangue is complex and diverse, mainly including SiO_2, Al_2O_3, Fe_2O_3, CaO, MgO, Hg, As, Cr, and Cd [72]. The abundance of SiO_2, CaO, Fe_2O_3, and MgO in the study area is higher than other China soil abundance. In Table 7, PC1 shows strong loadings for MgO, CaO, Fe_2O_3, and SiO_2; PC2 shows strong positive loadings for Se and Cd; and Pb and PC6 show strong positive loadings for As. To a certain degree, these aspects prove that the high Se concentration in the study area is closely related to mining activities. From the synthetical view, Se enrichment in soils in the study area is principally affected by rock weathering, mining activities, and coal combustion.

4.5. Assessment of PTEs Contamination in Soil

4.5.1. Analysis of Pollution Characteristics of PTEs in Soil

Statistical analysis of PTEs was studied and compared with that in the world [73], and ECP [28] is shown in Table 8. The spatial distribution of PTEs concentration in soils of the research area is shown in Figure S1 (Supplementary Material). The average concentration of all PTEs is within the risk screening value in GB 15618-2018 standard for agricultural soil pollution risk control. The concentrations of Ni, Cu, Zn, Cd, and Pb exceed the corresponding background values of the World and ECP. The proportions of samples with PTEs Cr, Ni, Cu, Zn, As, Cd, and Pb exceeding ECP background value are 26%, 64%, 52%, 72%, 0%, 95%, and 78%, respectively, which indicates that PTEs accumulate in different degrees in the soil of the study area. The coefficient of variation in Cr, Ni, Zn, As, Cd, and Pb is between 10% and 90%, showing moderate variability. The highest coefficient of variation in Cu is 98%, indicating a greater susceptibility of this element to staining across the study area compared to other trace metals [74]. It also demonstrates that Cu is originated from anthropogenic and human activity sources [75].

Table 8. Statistical description of PTEs concentration (μg/g).

	Cr	Ni	Cu	Zn	As	Cd	Pb
Mean	60.63	34.86	29.40	85.42	3.89	0.27	29.03
Median	60.20	31.45	23.17	73.93	3.67	0.24	27.13
Minimum	25.32	13.23	7.36	23.30	0.95	0.08	11.01
Maximum	129.57	278.15	360.96	253.72	8.49	1.29	99.83
Standard Deviation	11.47	22.01	28.81	37.10	1.43	0.14	9.49
Coefficient of variation (%)	19	63	98	43	37	52	33
World average data	42	18	14	62	4.7	1.1	25
ECP	65	30	23	64	10	0.12	23

4.5.2. Spatial Distribution Characteristics of PTEs in Soil

Inverse distance interpolation is carried out on the SFPI and NIPI of PTEs in soil, and the spatial distribution maps are shown in Figure 6. The order of average value of SFPI is Cd > Zn > Cu > Pb > Ni > Cr > As. As shown in Figure 6, heavy metal As of all samples in the study area is in degree I, which indicates that there is no As pollution risk. The risk of Cr pollution is negligible, as 74% of the area is in the safety domain, and 26% is in a slightly polluted domain. The distribution of Pb and Zn is similar; the safety domain appears in Cheng'an County and Linzhang County, while the seriously polluted domain clusters around Handan City. Overall, the eastern region performs much better than the western region, and the southern region performs significantly better than the northern region, according to the SFPI distribution of Cu. The high-value points of Cu are distributed in Wu'an City and Yongnian District. The pollution degree of Cd is the highest; only 5% of the area is in the safety domain, and slightly polluted, moderately polluted, and seriously polluted domains account for 44%, 36%, and 15%, respectively. The SFPI of Cd decreases to the surroundings with the Fengfeng as the center and shows a trend of high in the middle and low in the surroundings in the study area. According to the sample analysis, the majority of the area is in the safety and slightly polluted domain.

NIPI is a multi-factor environmental quality index approach that takes into account the maximum values to depict the overall contamination of PTEs in soil. The spatial distribution of NIPI is similar to that of SFPI of Cd, which is because NIPI highlights the influence and function of pollutants with the largest pollution index on environmental quality, that is, it highlights the heavy metal pollution with the most serious pollution degree, which causes Cd to occupy a large proportion in the comprehensive pollution index. The regions with NIPI greater than two are distributed in the central regions, such as Handan City and Fengfeng Mining District.

4.5.3. Source Analysis of Potential Toxic Pollution

The source apportionment of the two key groups of PTEs in the research area soil could be determined using Pearson correlation analysis (Table 6), Principal component analysis (Table 7), and a spatial distribution map (Figure 8): (1) Cr, Ni, Cu, Zn, and As, and (2) Cd and Pb.

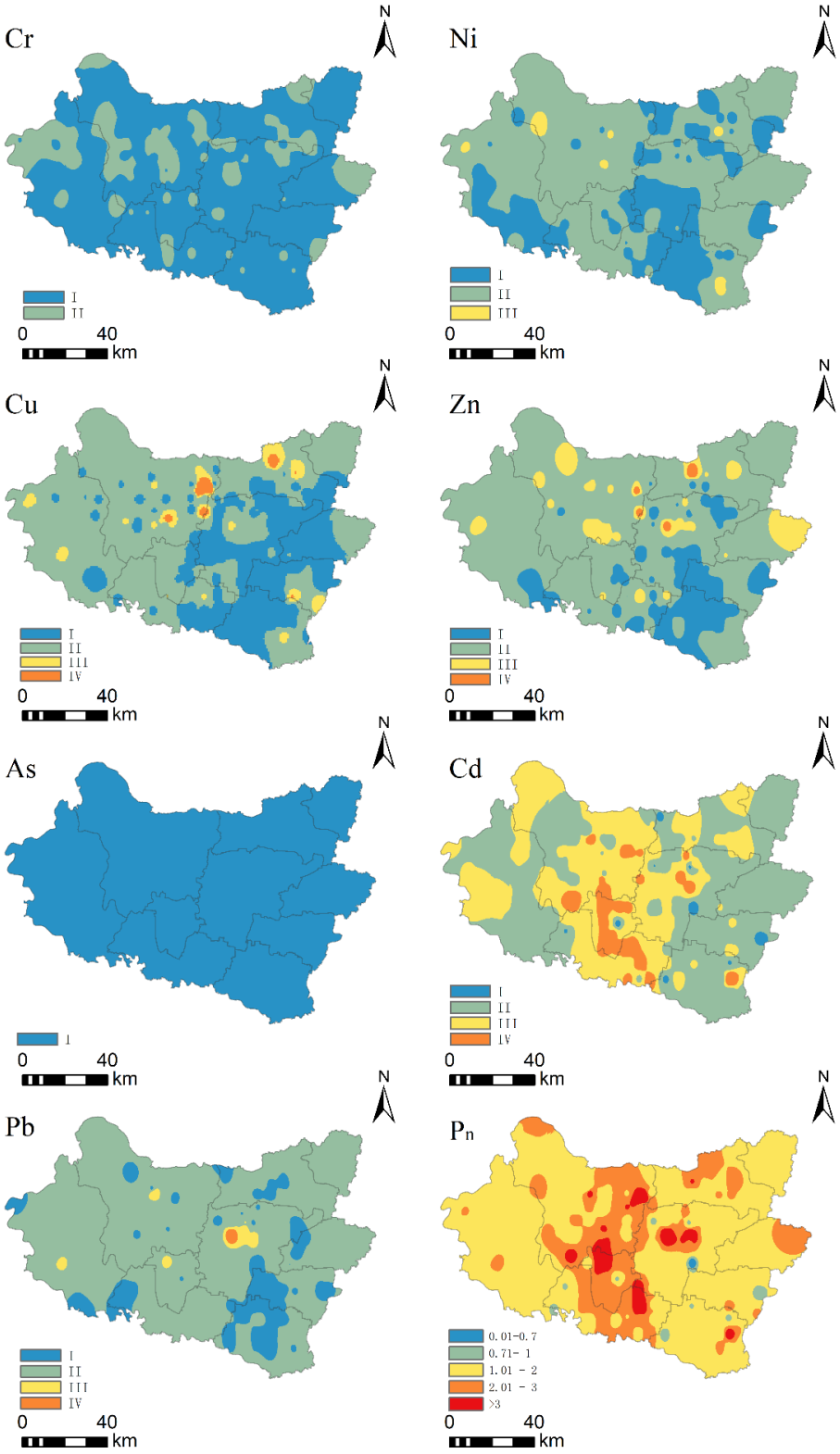

Figure 8. Distribution map of SFPI and NIPI of PTEs in soil.

Large amounts of mine waste (spoil) and dust emissions, which are elemental-rich industrial solid wastes, accumulate during the coal mining process. The soil around coal mines is high in Ni, Cu, and Zn, which could be owing to the natural weathering of the exposed spoils resulting in its degradation [76]. In addition, the burning of coal may also be a source of Cu, Ni, and Zn in soils around coal-fired power plants. Cr and As in soil are less contaminated by external sources and are most likely induced by natural processes such as weathering and erosion of sedimentary rocks [77]. Therefore, the first group is part of a mixed natural and anthropogenic source. Transportation (vehicle exhaust, lubricant use, tire wear, and road wear, etc.) was identified as a major source of PTEs contamination in soil [78]. Specifically, Pb is a critical component of gasoline and diesel, and Pb from vehicle exhaust can infiltrate the soil following atmospheric deposition [77]. Furthermore, Cd is a common component of agricultural products such as herbicides and fertilizers [79]. Industrial pollution is the main source of Pb and Cd. The second group originates from anthropogenic sources such as agricultural activities and industrial pollution.

5. Conclusions

In this study, we found that:

(1) Oxides higher than the reference values of China and ECP soils are CaO, Fe_2O_3, MgO, and P_2O_5, and elements with significantly higher background values are S, Se, and Ge, while elements that are significantly lower than the reference value such as As, Nb, Sn, and Hf. The analyzed results of total Se concentrations in soils of Handan area ranged from 0.00 to 1.95 μg/g with an average value of 0.45 μg/g, which exceeds the standard of Se-enrichment (0.4 μg/g) classified by Tan (1989) and is significantly higher than the average value of Se in China soil (0.29 μg/g) and Hebei Plain (0.21 μg/g).

(2) The concentration of Se in the central regions of the target area is noticeably higher than in the surrounding region. A continuous and irregular ring-like high Se-enrichment area is formed in Handan City, Yongnian District, Wu'an City, and Fengfeng Mining District, which is defined as a positive abnormal Se zone. Selenium positive anomaly zone in the study area is located in the hilly area in the west of Handan City and east of Taihang Mountains, and the plains near Handan City.

(3) EF values of Se vary greatly from 0.01 to 21.66, with an average of 5.06. The mean value of Se enrichment degree in each county is slight enrichment, the maximum EF of Se is in Fengfeng, while the minimum value is in Linzhang. The top nine EF mean values of trace elements are: S (14.87) > Se (4.97) > Ge (3.37) > Cd (2.99) > Sb (1.77) > Pb (1.71) > Li (1.38) > Cs (1.36) > Rb (1.36).

(4) The correlation coefficient between Se concentration and pH values suggests that pH is not the primary determinant of Se concentration distribution in the study area. Additionally, there is a significantly positive correlation between TOC and Se concentration; Cd, Pb, and Zn show a significantly positive correlation with Se. The result of PCA shows that Se concentration in the topsoil of Handan is affected synthetically by siderophile and chalcophile Cd, Pb, Fe_2O_3, and As.

(5) Comprehensively, PCA results and Source apportionment suggest that Se enrichment in soils is principally affected by weathering and leaching of parent material, mining activities, and coal combustion.

(6) As far as SFPI is concerned, most of the study areas are in the safety domain and slightly polluted domain and are at low ecological risk. The spatial distribution of NIPI is similar to that of SFPI of Cd, owing to highlights the heavy metal pollution with the most serious pollution degree. According to NIPI, the moderately and seriously polluted domain are distributed in Handan City, Fengfeng Mining District, and other central areas. The source apportionment of PTEs in the soil falls into two groups: (1) Cr, Ni, Cu, Zn, and As; (2) and Cd, and Pb. The first group is a component of a mixed source of both natural and anthropogenic. The second group originates from anthropogenic sources such as agricultural activities and industrial pollution.

Supplementary Materials: The following supporting information can be downloaded at: https://www.mdpi.com/article/10.3390/su14063183/s1, Figure S1: Spatial distribution of PTEs concentration in soils of the research area, Table S1: Major elements of soil samples (unit: %), Table S2: Trace elements of soil samples (unit: μg/g), Table S3: pH and TOC values in soil samples.

Author Contributions: Conceptualization, J.M. and S.J.; methodology, Y.H.; software, S.J. and Y.H.; validation, H.N., J.W. and M.Z.; investigation, J.M. and B.P.; resources, B.P.; data curation, M.Z.; writing—original draft preparation, H.H.; writing—review and editing, H.H., M.Z. and B.P.; supervision, J.W. and H.N.; project administration, J.W. and Y.S.; funding acquisition, J.W., H.N. and Y.S. All authors have read and agreed to the published version of the manuscript.

Funding: This research was funded by the National Natural Science Foundation of China, grant number: 41807305 and 41872173, the Hebei Provincial Natural Science Foundation, China, grant number: E2020209074 and D2021402022.

Institutional Review Board Statement: Not applicable.

Informed Consent Statement: Not applicable.

Data Availability Statement: Not applicable.

Acknowledgments: This research was financially supported by the National Natural Science Foundation of China, grant numbers: 41807305 and 41872173, the Hebei Provincial Natural Science Foundation, China, grant numbers: E2020209074 and D2021402022. The authors would like to thank Wenmu Guo, Haiping Zhao, and Lishu Wang from the Hebei University of Engineering, for their guidance and assistance in the process of HG-AFS, ICP-MS, and ICP-OES analysis, as well as Ruirui Ren and Ao Zhao for assistance in the experiment and software.

Conflicts of Interest: The authors declare no conflict of interest.

References

1. Fordyce, F.M. Selenium Deficiency and Toxicity in the Environment. In *Essentials of Medical Geology*; Selinus, O., Ed.; Springer: Dordrecht, The Netherlands, 2013; pp. 375–416. [CrossRef]
2. Mao, J.; Pop, V.J.; Bath, S.C.; Vader, H.L.; Redman, C.W.G.; Rayman, M.P. Effect of low-dose selenium on thyroid autoimmunity and thyroid function in UK pregnant women with mild-to-moderate iodine deficiency. *Eur. J. Nutr.* **2016**, *55*, 55–61. [CrossRef] [PubMed]
3. Izquierdo, A.; Casas, C.; Herrero, E. Selenite-induced cell death in Saccharomyces cerevisiae: Protective role of glutaredoxins. *Microbiology* **2010**, *156*, 2608–2620. [CrossRef] [PubMed]
4. Papp, L.V.; Lu, J.; Holmgren, A.; Khanna, K.K. From selenium to selenoproteins: Synthesis, identity, and their role in human health. *Antioxid. Redox Signal.* **2007**, *9*, 775–806. [CrossRef]
5. Parker, D.R.; Feist, L.J.; Varvel, T.W.; Thomason, D.N.; Zhang, Y. Selenium phytoremediation potential of Stanleya pinnata. *Plant Soil* **2003**, *249*, 157–165. [CrossRef]
6. Shi, Z.; Pan, P.; Feng, Y.; Kan, Z.; Li, Z.; Wei, F. Environmental water chemistry and possible correlation with Kaschin-Beck Disease (KBD) in northwestern Sichuan, China. *Environ. Int.* **2017**, *99*, 282–292. [CrossRef]
7. Bajaj, M.; Eiche, E.; Neumann, T.; Winter, J.; Gallert, C. Hazardous concentrations of selenium in soil and groundwater in North-West India. *J. Hazard. Mater.* **2011**, *189*, 640–646. [CrossRef] [PubMed]
8. WHO. *Guidelines for Drinking-Water Quality*; WHO: Geneva, Switzerland, 2011.
9. Mcneal, J.M.; Balistrieri, L.S. Geochemistry and occurrence of selenium: An overview. *Selenium Agric. Environ.* **1989**, *23*, 1–13. [CrossRef]
10. Dinh, Q.T.; Cui, Z.; Huang, J.; Tran, T.A.T.; Wang, D.; Yang, W.; Zhou, F.; Wang, M.; Yu, D.; Liang, D. Selenium distribution in the Chinese environment and its relationship with human health: A review. *Environ. Int.* **2018**, *112*, 294–309. [CrossRef]
11. Wang, R.; Yu, T.; Zeng, Q.; Yang, Z. Distribution characteristics, origin and influencing factors of soil selenium concentration of main farming areas in China. *Curr. Biotechnol.* **2017**, *7*, 359–366, (In Chinese with English Abstract). [CrossRef]
12. Li, Z. The Study on Source Tracking of Se Anomaly and Ecological Appraisal in Plain Terrain of Hebei. Ph.D. Thesis, Shijiazhuang University of Economics, Shijiazhuang, China, 2010. (In Chinese with English Abstract).
13. Zhang, X.; Ma, Z.; Guo, H.; Wang, S.M.; Li, J.; Li, H.; Gao, H. Investigation report on multi-target regional geochemistry in Hebei plain area. *Hebei Provincial Geological Survey Institute.* **2009**, *7*, 2, (In Chinese with English Abstract).
14. Zhang, X.; Ma, Z.; Wang, Y.; Wang, Z. The origin and ecological effects of selenium abnormity in soil im Hebei Plain. *Earth Environ.* **2012**, *40*, 541–547, (In Chinese with English Abstract). [CrossRef]
15. Rawlins, B.G.; McGrath, S.P.; Scheib, A.J.; Breward, N.; Cave, M.; Lister, T.R.; Ingham, M.; Gowing, C.; Carter, S. *The Advanced Soil Geochemical Atlas of England and Wales*; British Geological Survey: Nottingham, UK, 2012; 227p.

16. Ni, R.; Luo, K.; Tian, X.; Yan, S.; Zhong, J.; Liu, M. Distribution and geological sources of selenium in environmental materials in Taoyuan County, Hunan Province, China. *Environ. Geochem. Health.* **2016**, *38*, 927–938. [CrossRef] [PubMed]
17. Long, J.; Luo, K. Trace element distribution and enrichment patterns of Ediacaran-early Cambrian, Ziyang selenosis area, Central China: Constraints for the origin of Selenium. *J. Geochem. Explor.* **2017**, *172*, 211–230. [CrossRef]
18. Feng, C.; Liu, S.; Coulson, I.M. Lithological and Si–O–S isotope geochemistry: Constraints on the origin and genetic environment of the selenium (Se)-rich siliceous rocks in Enshi, Hubei Province, China. *Acta Geochim.* **2021**, *40*, 89–105. [CrossRef]
19. Tan, J. *The Atlas of Endemic Diseases and their Environments in the People's Republic of China*; Science Press: Beijing, China, 1989. (In Chinese)
20. Wang, H.; Mo, X. An outline of the tectonic evolution of China. *Episodes J. Int. Geosci.* **1995**, *18*, 6–16. [CrossRef]
21. Yan, C. Landform and structure of Handan area. *J. Hebei Inst. Archit. Sci. Technol.* **2000**, *17*, 63–65, (In Chinese with English Abstract).
22. BGMRHB (Bureau of Geology and Mineral Resources of Hebei Province). *Regional Geology of Beijing, Tianjin and Hebei Province*; Geological Publishing House: Beijing, China, 1989.
23. Zheng, J.; Mao, J.; Chen, M.; Li, G.; Ban, C. Geological characteristics and metallogenic model of skarn iron deposits in the Handan-Xingtai area, southern Hebei, China. *Geol. Bull. China.* **2007**, *26*, 150–154, (In Chinese with English Abstract).
24. Luo, K. Arsenic and fluorine contents and distribution patterns of early Paleozoic stonelike coal in the Daba Fold Zone and Yangtze Plate, China. *Energy Fuels* **2011**, *25*, 4479–4487. [CrossRef]
25. Tian, X.; Luo, K. Selenium, arsenic and molybdenum variation and bio-radiation in the Ediacaran-Cambrian interval. *Precambrian Res.* **2017**, *292*, 378–385. [CrossRef]
26. Niu, C.; Luo, K. Relationship of selenium, arsenic and sulfur in soil and plants in Enshi County, China. *J. Food Agric. Environ.* **2011**, *9*, 646–651.
27. Xing, Y.; Liu, Y.; Liang, P.; Liao, Q.; Pan, L.; Chen, J.; Huang, T.; Jiang, Z. Effects of phosphorus on selenium uptake of pakchoi and soil selenium morphology in Se-rich latosolic red soil and red soil. *Soils* **2018**, *50*, 1170–1175, (In Chinese with English Abstract). [CrossRef]
28. Zhu, L.; Ma, M.; Wang, Z. Soil eco-geochemical baseline in alluvial plains of eastern China. *Geol. China* **2006**, *33*, 1400–1405.
29. Nemerow, N.L. *Scientific Stream Pollution Analysis*; Scripta Book, Co.: Hagerstown, MD, USA, 1974.
30. Cheng, J.; Zhou, S.; Zhu, Y. Assessment and mapping of environmental quality in agricultural soils of Zhejiang Province, China. *J. Environ. Sci.* **2007**, *19*, 50–54. [CrossRef]
31. Gong, G.; Mattevada, S.; O'bryant, S.E. Comparison of the accuracy of kriging and IDW interpolations in estimating groundwater arsenic concentrations in Texas. *Environ. Res.* **2014**, *130*, 59–69. [CrossRef]
32. Yan, M.; Gu, T.; Chi, Q.; Wang, C. Abundance of chemical elements of soils in China and supergenesis geochemistry characteristics. *Geophys. Geochem. Explor.* **1997**, *21*, 161–167, (In Chinese with English Abstract).
33. Liu, Z. Soil trace elements in China. *Adv. Earth Sci.* **1998**, *13*, 589. (In Chinese)
34. Zhang, H.; Luo, Y.; Wu, L.; Zhang, G.; Zhao, Q.; Huang, M. Hong Kong soil researches II. distribution and content of Selenium in soil. *Acta Pedol. Sin.* **2005**, *42*, 404–410, (In Chinese with English Abstract).
35. Zhang, X.; Wen, H.; Cai, L.; Luo, J.; Mu, G.; Wang, Q.; Jiang, H.; Wang, S. Distribution of Selenium and Its Influencing Factors in Soils of Jiedong Area, Guangdong Province. *Environ. Sci. Technol.* **2019**, *42*, 189–196. [CrossRef]
36. Liu, Y.; Tian, X.; Liu, R.; Liu, S.; Zuza, A.V. Key driving factors of selenium-enriched soil in the low-se geological belt: A case study in red beds of sichuan basin, China. *Catena* **2021**, *196*, 104926. [CrossRef]
37. Zhu, J.; Wang, N.; Li, S.; Li, L.; Su, H.; Liu, C. Distribution and transport of selenium in Yutangba, China: Impact of human activities. *Sci. Total Environ.* **2008**, *392*, 252–261. [CrossRef]
38. Rudnick, R.L.; Gao, S.; Holland, H.D. Composition of the continental crust. *Crust* **2003**, *3*, 1–64.
39. Alfthan, G.; Eurola, M.; Ekholm, P.; Venäläinen, E.; Root, T.; Korkalainen, K.; Hartikainen, H.; Salminen, P.; Hietaniemi, V.; Aspila, P.; et al. Effects of nationwide addition of selenium to fertilizers on foods, and animal and human health in Finland: From deficiency to optimal selenium status of the population. *J. Trace Elem. Med. Biol.* **2015**, *31*, 142–147. [CrossRef] [PubMed]
40. Cartes, P.; Gianfreda, L.; Mora, M. Uptake of selenium and its antioxidant activity in ryegrass when applied as selenate and selenite forms. *Plant Soil* **2005**, *276*, 359–367. [CrossRef]
41. Xiao, K.; Tang, J.; Chen, H.; Li, D.; Liu, Y. Impact of land use/land cover change on the topsoil selenium concentration and its potential bioavailability in a karst area of southwest China. *Sci. Total Environ.* **2020**, *708*, 135201. [CrossRef] [PubMed]
42. Ngigi, P.B.; Laing, D.G.; Masinde, P.W.; Lachat, C. Selenium deficiency risk in central Kenya highlands: An assessment from the soil to the body. *Environ. Geochem. Health* **2020**, *42*, 2233–2250. [CrossRef]
43. Matos, R.P.; Lima, V.M.; Windmöller, C.C.; Nascentes, C.C. Correlation between the natural levels of selenium and soil physico-chemical characteristics from the Jequitinhonha Valley (MG), Brazil. *J. Geochem. Explor.* **2017**, *172*, 195–202. [CrossRef]
44. Nakamaru, Y.M.; Altansuvd, J. Speciation and bioavailability of selenium and antimony in non-flooded and wetland soils: A review. *Chemosphere* **2014**, *111*, 366–371. [CrossRef]
45. Li, J.; Peng, Q.; Liang, D.L.; Liang, S.J.; Chen, J.; Sun, H.; Li, S.Q.; Lei, P.H. Effects of aging on the fraction distribution and bioavailability of selenium in three different soils. *Chemosphere* **2016**, *144*, 2351–2359. [CrossRef]
46. Wang, C.; Ji, J.; Zhu, F. Characterizing Se transfer in the soil-crop systems under field condition. *Plant Soil* **2017**, *415*, 535–548. [CrossRef]

47. Wang, H.; Luo, J.; Cai, L.; Mu, G.; Wang, Q.; Jiang, H.; Wang, S.; He, M. Distribution of selenium and its influencing factors in soils of Huilai county, Guangdong Province. *Chin. J. Agric. Resour. Reg. Plan.* **2020**, *41*, 262–269, (In Chinese with English Abstract).
48. Hao, L.; Zhang, J.; Zhang, S.; Ma, S.; Li, B.; Long, J.; Fan, J.; Luo, K. Distribution characteristics and main influencing factors of selenium in surface soil of natural selenium-rich area: A case study in Langao County, China. *Environ. Geochem. Health* **2021**, *43*, 333–346. [CrossRef] [PubMed]
49. Yuan, B.; Feng, Y.; Li, S.; Lu, G.; You, J.; Xiao, F. Analysis on the Causes and Influencing Factors of Selenium-Rich Soil in Sinan County. *China Resour. Compr. Util.* **2021**, *39*, 63–68, (In Chinese with English Abstract).
50. Xu, Y.; Li, Y.; Li, H.; Wang, L.; Liao, X.; Wang, J.; Kong, C. Effects of topography and soil properties on soil selenium distribution and bioavailability (phosphate extraction): A case study in Yongjia County, China. *Sci. Total Environ.* **2018**, *633*, 240–248. [CrossRef] [PubMed]
51. Tan, J.; Zhu, W.; Wang, W.; Li, R.; Hou, S.; Wang, D.; Yang, L. Selenium in soil and endemic diseases in China. *Sci. Total Environ.* **2002**, *284*, 227–235. [CrossRef]
52. Fakour, H.; Lin, T.; Lo, S. Equilibrium modeling of arsenic adsorption in a ternary arsenic–iron oxide–natural organic matter system. *Clean Soil Air Water* **2016**, *44*, 1287–1295. [CrossRef]
53. Li, X.; Gao, N.; Zhao, W.; Liu, Z. Distribution characteristics of selenium in cultivated soil and its influencing factors in Qingtongxia City of Ningxia. *J. Agric. Resour. Environ.* **2018**, *35*, 422–429, (In Chinese with English Abstract). [CrossRef]
54. Chen, R.; Zhang, L.; Wu, Y.; Qiu, L. Soil Profi le Weathering Feature of Eroded Weathering Granite Slope at Different Sections. *Acta Pedol. Sin.* **2016**, *53*, 1380–1388, (In Chinese with English Abstract).
55. Yu, T.; Yang, Z.; Lv, Y.; Hou, Q.; Xia, X.; Feng, H.; Zhang, M.; Jin, L.; Kan, Z. The origin and geochemical cycle of soil selenium in a Se-rich area of China. *J. Geochem. Explor.* **2014**, *139*, 97–108. [CrossRef]
56. Xia, F.; Zhang, X.; Yang, Y.; Chen, P.; Liu, B. Geochemical characteristics and influencing factors of selenium in soils and agricultural products in Ningguo City, Anhui Province. *Soils* **2021**, *53*, 585–593, (In Chinese with English Abstract). [CrossRef]
57. Nakamura, K.; Kuwatani, T.; Kawabe, Y.; Komai, K. Extraction of heavy metals characteristics of the 2011 Tohoku tsunami deposits using multiple classification analysis. *Chemosphere* **2016**, *144*, 1241–1248. [CrossRef]
58. Fang, X.; Peng, B.; Wang, X.; Song, Z.; Zhou, D.; Wang, Q.; Qin, Z.; Tan, C. Distribution, contamination and source identification of heavy metals in bed sediments from the lower reaches of the Xiangjiang River in Hunan province, China. *Sci. Total Environ.* **2019**, *689*, 557–570. [CrossRef] [PubMed]
59. Tribovillard, N.; Algeo, T.J.; Lyons, T.; Riboulleau, A. Trace metals as paleoredox and paleoproductivity proxies: An update. *Chem. Geol.* **2006**, *232*, 12–32. [CrossRef]
60. Brügmann, G.; Naldrett, A.; Asif, M.; Lightfoot, P.C.; Gorbachev, N.S.; Fedorenko, V.A. Siderophile and chalcophile metals as tracers of the evolution of the Siberian Trap in the Noril'sk region, Russia. *Geochim. Cosmochim. Acta* **1993**, *57*, 2001–2018. [CrossRef]
61. Rosenfeld, I.; Beath, O.A. *Selenium: Geobotany, Biochemistry, Toxicity, and Nutrition*; Academic Press: Cambridge, MA, USA, 2013.
62. Wang, Z.; Gao, Y. Biogeochemical cycling of selenium in Chinese environments. *Appl. Geochem.* **2001**, *16*, 1345–1351. [CrossRef]
63. Zhang, M.; Sun, Y. Source of selenium in Handan geochemical anomaly belt: Evidences from petrology and geochemistry of Upper Paleozoic in western Handan, China. *J. Geochem. Explor.* **2021**, *226*, 106770. [CrossRef]
64. Long, J.; Zhang, S.; Luo, K. Selenium in Chinese coal gangue: Distribution, availability, and recommendations. *Resour. Conserv. Recycl.* **2019**, *149*, 140–150. [CrossRef]
65. Bullock, L.A.; Parnell, J.; Perez, M.; Armstrong, J.G.; Feldmann, J.; Boyce, A.J. High selenium in the carboniferous coal measures of Northumberland, North East England. *Int. J. Coal Geol.* **2018**, *195*, 61–74. [CrossRef]
66. Zhao, Y. Study on the Genesis and Utilization of Selenium Rich Soil in Handan and Xingtai Area. Master's Thesis, Hebei GEO University, Shijiazhuang, China, 2020. (In Chinese with English Abstract). [CrossRef]
67. Rzymski, P.; Klimaszyk, P.; Marszelewski, W.; Borowiak, D.; Mleczek, M.; Nowiński, K.; Pius, B.; Niedzielski, P.; Poniedziałek, B. The chemistry and toxicity of discharge waters from copper mine tailing impoundment in the valley of the Apuseni Mountains in Romania. *Environ. Sci. Pollut. Res.* **2017**, *24*, 21445–21458. [CrossRef]
68. Hussain, R.; Wei, C.; Luo, K. Hydrogeochemical characteristics, source identification and health risks of surface water and groundwater in mining and non-mining areas of Handan, China. *Environ. Earth Sci.* **2019**, *78*, 402. [CrossRef]
69. Wen, H.; Carignan, J. Reviews on atmospheric selenium: Emissions, speciation and fate. *Atmos. Environ.* **2007**, *41*, 7151–7165. [CrossRef]
70. Bañuelos, G.; Roche, J.D.; Robinson, J. Developing selenium-enriched animal feed and biofuel from canola planted for managing Se-laden drainage waters in the Westside of Central California. *Int. J. Phytoremediation* **2010**, *12*, 243–254. [CrossRef] [PubMed]
71. Song, T.; Cui, G.; Su, X.; He, J.; Tong, S.; Liu, Y. The origin of soil selenium in a typical agricultural area in Hamatong River Basin, Sanjiang Plain, China. *Catena* **2020**, *185*, 104355. [CrossRef]
72. The Group of Environmental and Endemic Diseases. The relation of Keshan disease to the natural environment and the background of selenium nutrition. *Acta Nutr. Sin.* **1982**, *4*, 175–182, (In Chinese with English Abstract).
73. Alloway, B.J. Sources of Heavy Metals and Metalloids in Soils. In *Heavy Metals in Soils*; Springer: Dordrecht, The Netherlands, 2013; pp. 11–50.
74. Siddiqui, A.U.; Jain, M.K.; Masto, R.E. Pollution evaluation, spatial distribution, and source apportionment of trace metals around coal mines soil: The case study of eastern India. *Environ. Sci. Pollut. Res.* **2020**, *27*, 10822–10834. [CrossRef]

75. Zhou, M.; Liao, B.; Shu, W.; Yang, B.; Lan, C. Pollution assessment and potential sources of heavy metals in agricultural soils around four Pb/Zn mines of Shaoguan city, China. *Soil Sediment Contam. Int. J.* **2015**, *24*, 76–89. [CrossRef]
76. Masto, R.E.; Ram, L.C.; George, J.; Selvi, V.A.; Sinha, A.K.; Verma, S.K. Status of some soil trace elements and their potential human health risks around a coal beneficiation plant. *Int. J. Coal Prep. Util.* **2011**, *31*, 61–77. [CrossRef]
77. Wei, P.; Shao, T.; Wang, R.; Chen, Z.; Zhang, Z.; Xu, Z.; Zhu, Y.; Li, D.; Fu, L.; Wang, F. A study on heavy metals in the surface soil of the region around the Qinghai Lake in Tibet Plateau: Pollution risk evaluation and pollution source analysis. *Water* **2020**, *12*, 3277. [CrossRef]
78. Wang, G.; Zeng, C.; Zhang, F.; Zhang, Y.; Scott, C.A.; Yan, X. Traffic-related trace elements in soils along six highway segments on the Tibetan Plateau: Influence factors and spatial variation. *Sci. Total Environ.* **2017**, *581*, 811–821. [CrossRef]
79. Wang, S.; Cai, L.; Wen, H.; Luo, J.; Wang, Q.; Liu, X. Spatial distribution and source apportionment of heavy metals in soil from a typical county-level city of Guangdong Province, China. *Sci. Total Environ.* **2019**, *655*, 92–101. [CrossRef]